Proceedings of the CERN-BINP Workshop for Young Scientists in e^+e^- Colliders, Geneva, Switzerland, 22 – 25 August 2016, edited by V. Brancolini ans L. Linssen, CERN Proceedings, Vol. 1/2017, CERN-Proceedings-2017-001 (CERN, Geneva, 2017)

Kaon Identification using the Tracking System of the CMD-3 Detector

R.R. Akhmetshin, A.N. Amirkhanov, A.V. Anisenkov, V.M. Aulchenko, V.Sh. Banzarov, N.S. Bashtovoy, A.E. Bondar, A.V. Bragin, S.I. Eidelman, D.A. Epifanov, L.B. Epshteyn, A.L. Erofeev, G.V. Fedotovich, S.E. Gayazov, A.A. Grebenuk, S.S. Gribanov, D.N. Grigoriev, F.V. Ignatov, V.L. Ivanov, S.V. Karpov, V.F. Kazanin, O.A. Kovalenko, A.A. Korobov, A.N. Kozyrev, E.A. Kozyrev, P.P. Krokovny, A.E. Kuzmenko, A.S. Kuzmin, I.B. Logashenko, P.A. Lukin, K.Yu. Mikhailov, V.S. Okhapkin, Yu.N. Pestov, A.S. Popov, G.P. Razuvaev, A.A. Ruban, N.M. Ryskulov, A.E. Ryzhenenkov, V.E. Shebalin, D.N. Shemyakin, B.A. Shwartz, A.L. Sibidanov, E.P. Solodov, V.M. Titov, A.A. Talyshev, A.I. Vorobiov, Yu.V. Yudin*
Budker Institute of Nuclear Physics, SB RAS, Novosibirsk, 630090, Russia

Abstract
This paper describes the K/π separation technique based on ionisation losses in the drift chamber of the CMD-3 detector. First the procedure of the ionisation-loss calibration is described. Then methods of K/π separation are discussed for the example process $e^+e^- \to K^+K^-\pi^+\pi^-$.

Keywords
Drift chamber; Ionisation losses calibration; VEPP-2000; CMD-3 detector.

1 Introduction

The electron-positron collider VEPP-2000 [1] was commissioned at the Budker Institute of Nuclear Physics (BINP) in 2010. The machine covers a center-of-mass energy range from $E = 0.32$ GeV to 2 GeV and employs a novel so-called round beam technique to reach luminosities of up to $10^{32}\,\mathrm{cm}^{-2}\mathrm{s}^{-1}$ at 2 GeV.

The CMD-3 [2] detector occupies one of two interaction regions of VEPP-2000. The detector layout is shown in Fig. 1. The tracks of charged particles are detected by the cylindrical drift chamber (DC) with hexagonal cells. The fiducial volume for charged tracks is precisely determined by the Z-chamber, a Multi Wire Proportional Chamber (MWPC) with dual anode and cathode readout. The barrel electromagnetic calorimeter, placed outside of the superconducting solenoid (0.08 X_0, 13 T), consists of two systems: the Liquid Xenon (LXe) calorimeter (about 5.4 X_0) and the Cesium Iodine (CsI) crystal calorimeter (about 8.1 X_0)) that surrounds the LXe calorimeter. The LXe calorimeter has 7 layers and utilizes dual readout: the anode signals are used for measurement of the total energy deposition while signals from the cathode strips provide information about the shower profile. Also they are used for the measurement of the coordinates of photons with high precision (about 1-2 mm). The endcap Bismuth Germanate (BGO) crystal calorimeter (about 13.4 X_0) operates in the main magnetic field. The Time-Of-Flight (TOF) system, designed to identify the particle species, is placed between the two layers of the barrel calorimeter. The calorimeters are surrounded by the so-called muon range system based on scintillation counters. The full detector has a radius of 1.5 m and a length of 2 m.

During the first experimental run from 2010 to 2013, the detector has collected about 60 pb^{-1} of integrated luminosity. An average luminosity above $10^{31}\,\mathrm{cm}^{-2}\mathrm{s}^{-1}$ was reached at VEPP-2000, which is still below the design luminosity. The main limitation at high energies was a deficit of positrons. After the VEPP-2000 upgrade, started in 2013, which included the commissioning of the new positron injection facility and an increase of the maximum energy of the booster ring, one of the pre-accelerators, a gain in the maximum luminosity of up to a factor of 10 is expected.

The main task of the CMD-3 detector is the measurement of the exclusive cross sections of the electron-positron annihilation into hadrons. For the measurement of events including charged kaons

*Corresponding author. Email: dimnsh@yandex.ru

https://doi.org/10.23727/CERN-Proceedings-2017-001.159

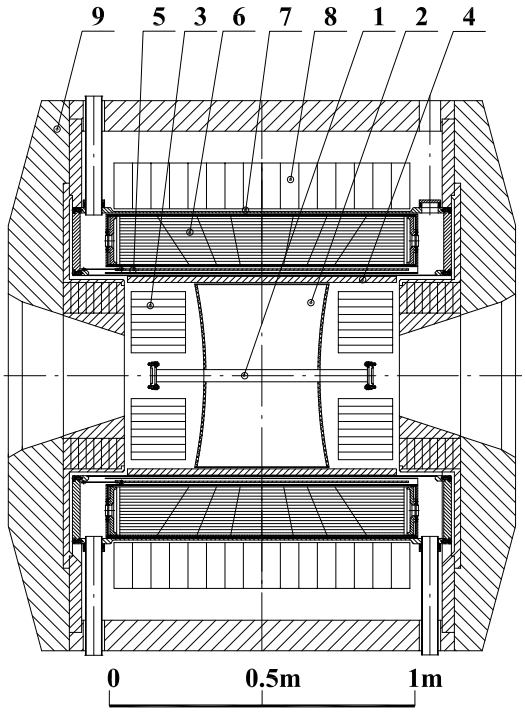

Fig. 1: CMD-3 detector: 1 – beam pipe, 2 – drift chamber, 3 – BGO calorimeter, 4 – Z-chamber, 5 – SC solenoid ($0.08X_0$, 13 T), 6 – LXe calorimeter, 7 – TOF system, 8 – CsI calorimeter, 9 – yoke. Outer muon range system is not shown.

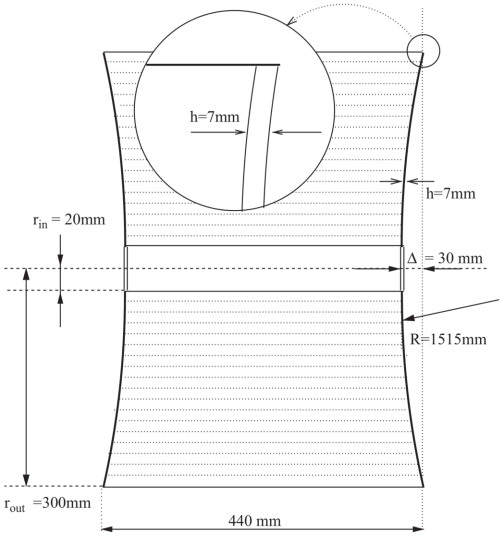

Fig. 2: Drift chamber layout.

a kaon identification procedure is needed, where pions represent the largest background. This paper describes the method of K/π separation using ionisation losses (dE/dx) in the DC and the calibration of the dE/dx measurement with the DC.

2 Drift chamber

The drift chamber is the main tool of the CMD-3 detector for charged particle reconstruction. A sketch of the DC is shown in Fig. 2. 1218 identical hexagonal cells of a cell side of 9 mm and a sense to field wires ratio of 1:2 cover the full sensitive volume of the chamber. The charge division technique is used to measure the coordinate along the sense wires which have 15 mm diameter and are made of gold plated tungsten-rhenium alloy with a resistance of 1 kΩm. The field wires have a diameter of 100 mm and they are made of titanium. The DC end plates are 7 mm thick spherical segments made of carbon fibers. As gas mixture Ar:C_4H_{10} is used with a proportion of 80:20. A simulation with Garfield [3] has shown a maximum drift time in the 1.3 T magnetic field of about 600 ns while the beam revolution time is 80 ns. The mixture is prepared using two Bronkhorst gas flow controllers. Direct measurements of the magnetic field in the DC volume have shown an agreement with calculations: the maximum deviation of the magnetic field does not exceed 1% along the beam axis and 0.2% from the interaction point to the outer shell.

3 Ionisation losses calibration

Cosmic muon events are used for the estimation of the DC gain for each wire. Also the reconstructed track parameters allow one to know the position at which a particle crosses a cell and calculate a geometrical amendment for the collected ionization. The calibration includes corrections on the following

parameters:

- distance from track to the wire ρ,
- polar angle of track θ,
- longitudinal position of the track z,
- amplitude difference between wires.

As shown in Fig. 3, the ionisation losses is constant for central values of z while at the borders of the DC it shows a linear dependence on the longitudinal track position. The dE/dx dependence on the distance between track and wire (ρ) is different for different polar angles (see Fig.4). Hence, the mean ionisation loss as a function of the polar angle (see Fig. 5) are approximated for different values of ρ. These approximations are then used for the detector calibration.

For the calibration of the dE/dx scale, we use "one-proton" events with a momentum of 350 MeV/c and cosmic muon events with a momentum of higher than 500 MeV/c. The mean dE/dx measured with the wires of DC is presented in Fig. 6. Red points correspond to protons, blue points correspond to cosmic muon events. We set mean ionisation losses value on 10000 arbitrary units for protons and 2000 arbitrary units for cosmic muon events. The final dE/dx measurement resolution is 10%-13% for minimum ionisation particles.

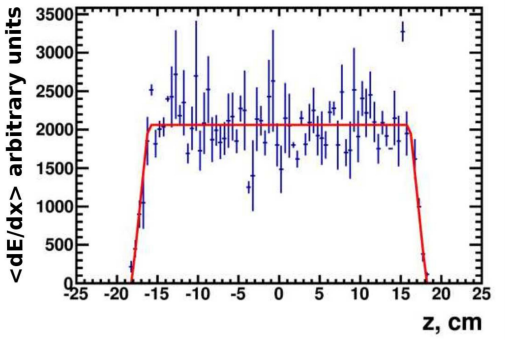

Fig. 3: Dependence of the mean dE/dx on the longitude position of track z.

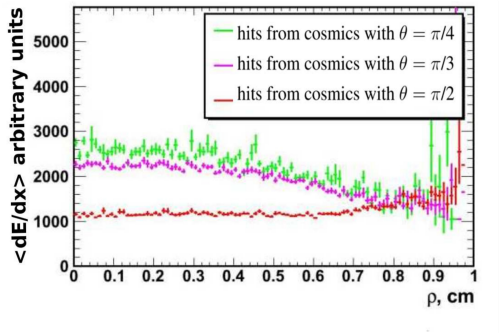

Fig. 4: Dependence of the mean dE/dx on the distance between track and wire ρ for three different polar angles.

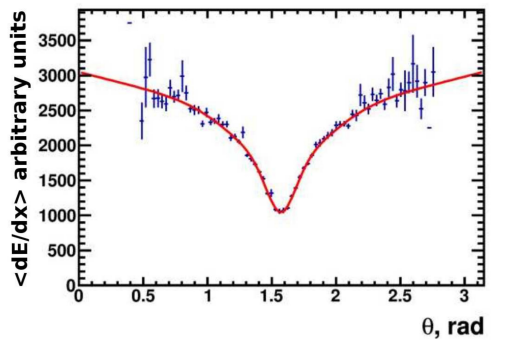

Fig. 5: Dependence of the mean dE/dx on the polar angle of track θ.

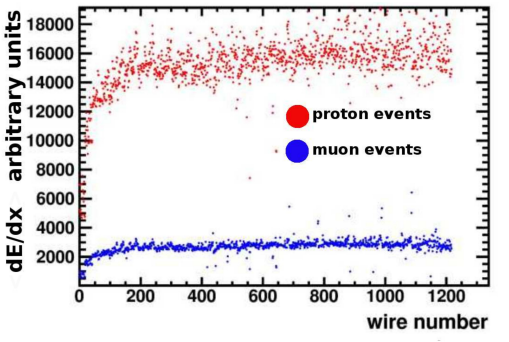

Fig. 6: dE/dx for all wires of the DC for proton events and cosmic muon events.

4 Kaon identification

The dE/dx distribution for collinear events (two tracks with $\Delta\theta = 0.15$ rad and $\Delta\phi = 0.1$ rad) at $E = 1.019$ GeV is presented in Fig. 7. The momentum of kaons are about 110 MeV/c. A cut based event selection shown as black lines allows to identify events of the process $e^+e^- \to K^+K^-$ with less than 0.5% background [4].

The dE/dx in the DC versus the particle momentum for $e^+e^- \to K^+K^-\pi^+\pi^-$ events is presented in Fig. 8 for $E = 1.8$ GeV. For the K/π separation for particles with a momentum of larger than 400 MeV/c, a probability density function (PDF) with momentum and dE/dx dependence is used to extract the number of pions and kaons in the event. It is constructed for kaons f_K(p,dE/dx) and pions f_π(p,dE/dx) as

$$f_{K,\pi}(\mathrm{p}, \mathrm{dE/dx}) = \mathrm{N}_G \times G(< \mathrm{dE/dx} >, \sigma_G) + \mathrm{N}_{Gl} \times Gl(< \mathrm{dE/dx} >, \sigma_{Gl}, \eta). \quad (1)$$

where $G(< \mathrm{dE/dx} >, \sigma_G)$ is the Gaussian function, $Gl(< \mathrm{dE/dx} >, \sigma_{Gl}, \eta)$ is the logarithmic Gaussian function. The latter is necessary to describe the tails of the distribution of the ionization losses. The average ionization losses <dE/dx>, standard deviations σ_G and σ_{Gl}, asymmetry η, amplitudes N_{Gl} and N_G depend only on the particle momentum. The PDF parameters are extracted from the dE/dx dependence on the particle momentum using a 7-dim. fit. First the f_π(p,dE/dx) is determined using a sample of $e^+e^- \to \pi^+\pi^-\pi^+\pi^-$ events, then the f_K(p,dE/dx) is determined using a sample of $e^+e^- \to K^+K^-\pi^+\pi^-$ events with fixed f_π(p,dE/dx). This procedure was performed for simulated and experimental data at each energy point. An example of a PDF is shown in Fig. 9 for momenta of 400 - 450 MeV/c.

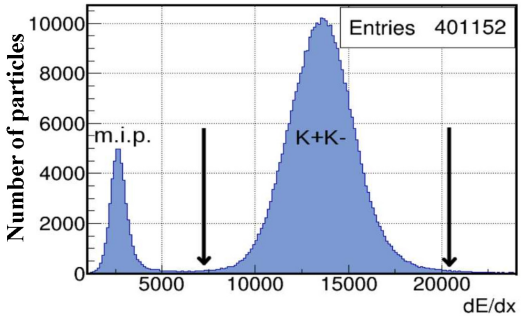

Fig. 7: Particle ionization losses in DC for collinear events at $E = 1.019$ GeV.

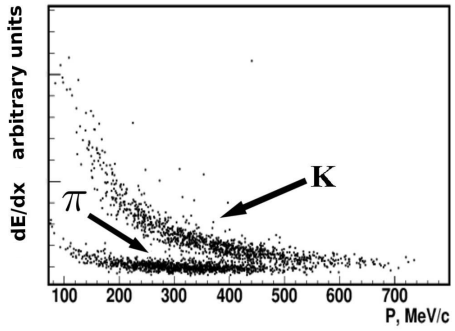

Fig. 8: Pion and kaon ionization losses in DC as a function of the particle momentum in simulation.

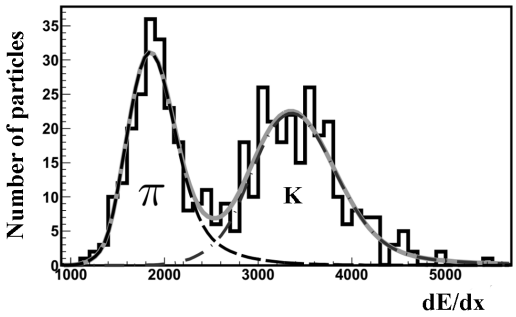

Fig. 9: Pion and kaon ionization losses in DC for the momentum interval from 400 to 450 MeV/c in simulation.

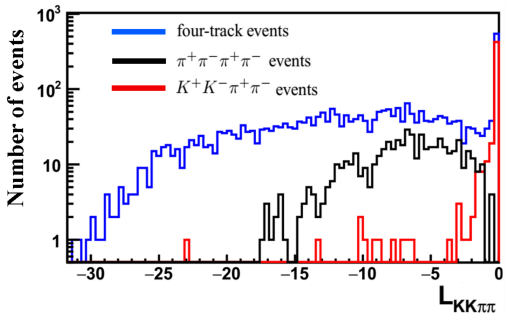

Fig. 10: Distribution of the likelihood function ($L_{KK\pi\pi}$) for the four-track events in simulation. The blue histogram corresponds to all four-track events, the black one to $\pi^+\pi^-\pi^+\pi^-$ events and the red one to $K^+K^-\pi^+\pi^-$ events.

In the analysis of the process $e^+e^- \to K^+K^-\pi^+\pi^-$ the likelihood function ($L_{KK\pi\pi}$) is defined as

$$L_{KK\pi\pi} = \log\Big(\frac{\prod_i f^i_{\alpha_i}(p, \mathrm{dE/dx})}{\prod_i [f^i_\pi(p, \mathrm{dE/dx}) + \mathrm{f^i_K(p, dE/dx)}]}\Big), \quad (2)$$

where i is the track index, α_i is the supposed type (K or π) of the particle corresponding to the ith track. The $L_{KK\pi\pi}$ is constructed for events with three or four tracks in the DC, so the track index changes from 1 to 3 or 4, respectively. $L_{KK\pi\pi}$ is constructed under the assumption that each event is a $K^+K^-\pi^+\pi^-$ event, so two tracks are identified as kaons and two as pions. Therefore, taking into account all the permutations and charges of the particles, $L_{KK\pi\pi}$ receives four different values for each event. The most probable combination of particle types provides a maximum of this function. The distribution of $L_{KK\pi\pi}$ for simulated data at a center-of-mass energy of 2 GeV is shown in Fig. 10. The blue histogram corresponds to all four-track events while the black and red ones correspond to $\pi^+\pi^-\pi^+\pi^-$ and $K^+K^-\pi^+\pi^-$ events respectively. It is seen that the likelihood function value also is a good parameter to select $e^+e^- \to K^+K^-\pi^+\pi^-$ events from background. The condition for the $L_{KK\pi\pi}$ value to be larger than -2 was chosen as a selection condition, which allows to suppress background events by a factor of 20 and it preserves more than 99% of signal events, according to simulation as extracted from Fig. 10. Similar likelihood functions were used for analyses of the processes $e^+e^- \to K^+K^-\omega$, $K^+K^-\pi$ and $K^+K^-\eta$ [6].

5 Conclusion

The CMD-3 tracking system based on the DC and Z-chamber participated in the data taking since 2010. Calibration procedures of the dE/dx measurement have been developed and they were used during all data taking periods. The DC ionisation losses resolution is 10%-13%. Information about ionisation losses in the DC is successfully used in analyses of processes $e^+e^- \to K^+K^-\omega$, $K^+K^-\pi$,$K^+K^-\pi^+\pi^-$ and $K^+K^-\eta$.

Acknowledgements

We wish to thank the VEPP-2000 personnel for the excellent machine operation. This work is supported in part by Russian Science Foundation (grant No. 14-50-00080), by the Russian Foundation for Basic Research grants RFBR 14-02-00580-a, RFBR 14-02-91332, RFBR 15-02-05674-a, RFBR 16-02-00160-a, RFBR 17-02-00897-a.

References

[1] Y.M. Shatunov *et al.*, *Conf. Proc. C* 0006262 (2000) 439. http://accelconf.web.cern.ch/accelconf/e00/PAPERS/MOP4A08.pdf

[2] B.I. Khazin *et al.*, *Nucl. Phys. Proc. Suppl.* 181-182 (2008) 376. https://doi.org/10.1016/j.nuclphysbps.2008.09.068

[3] Garfield - simulation of gaseous detectors. http://garfield.web.cern.ch/garfield/, last accessed April 21st 2017

[4] E.A. Kozyrev *et al.*, *Phys. Atom. Nucl.* 78 (2015) 358-362. https://doi.org/10.1134/S1063778815020192

[5] D.N. Shemyakin *et al.*, *Phys. Lett. B*756 (2016) 153-160. https://doi.org/10.1016/j.physletb.2016.02.072

[6] V.L. Ivanov *et al.*, *Phys. Atom. Nucl.* 79 (2016) 251-259. https://doi.org/10.1134/S1063778816020083